Lung Cancer 132 (2019) 59–64

Contents lists available at ScienceDirect

Lung Cancer

journal homepage: www.elsevier.com/locate/lungcan

Patients with SMARCA4-deficient thoracic sarcoma and severe skeletal-related events

Kei Kunimasa[a,1,*], Harumi Nakamura[b,1], Kazuko Sakai[c], Motohiro Tamiya[a], Madoka Kimura[a], Takako Inoue[a], Kazumi Nishino[a], Hanako Kuhara[a], Shin-ichi Nakatsuka[b], Kazuto Nishio[c], Fumio Imamura[d], Toru Kumagai[a]

[a] Department of Thoracic Oncology, Osaka International Cancer Institute, 3-1-69 Otemae Chuoku, Osaka City, Japan
[b] Department of Diagnostic Pathology and Cytology, Osaka International Cancer Institute, 3-1-69 Otemae Chuoku, Osaka City, Japan
[c] Department of Genome Biology, Kindai University Faculty of Medicine, Osaka-Sayama, Osaka, Japan
[d] Department of Clinical Oncology, Osaka International Cancer Institute, 3-1-69 Otemae Chuoku, Osaka City, Japan

ARTICLE INFO

Keywords:
SWI/SNF complex
SMARCA4
Lung cancer
Skeletal related event

ABSTRACT

Objectives: SMARCA4-deficient thoracic sarcoma(DTS) is a recently identified new entity of thoracic malignancies characterized by inactivation of *SMARCA4*. Patients with SMARCA4-DTS have a particulary aggresive clinical course and no effective treatments. However, the detailed clinical features of SMARCA4-DTS remain unclear. Here, we report the clinical courses and molecular profiles of two cases of SMARCA4-DTS.

Materials and Methods: We experienced strikingly similar two patients of SMARCA4-DTS. The clinicopathologic features were reviewed, and detailed immunohistochemical and comprehensive cancer panel analysis with next generation sequencing confirmed the diagnosis.

Results: Our cases had many clinical and radiological observations characteristic of SMARCA4-DTS in common. Immunohistochemical staing showed complete loss of SMARCA4 in tumor cells. Loss of function mutations were detected in *SMARCA4*. We found that severe SREs comprise a new significant clinical feature of SMARCA4-DTS.

Conclusion: Integrated clinico-radiologic–pathologic–genetic diagnosis is essential for SMARCA4-DTS and physicians should pay attention to severe SREs during the clinical course of this disease.

1. Introduction

SMARCA4 is one of the core catalytic subunits of the SWI/SNF complex and its inactivation has been reported in several aggressive tumors with high-grade undifferentiated rhabdoid morphology including small cell carcinoma of the ovary, hypercalcemic type (SCCOHT) [1]. Recent genetic analysis revealed a group of undifferentiated thoracic malignancies with SMARCA4 inactivation presenting as compressive tumors often involving the mediastinum, with or without lung involvement, and occurring in relatively young patients and displaying aggressive behavior with poor prognosis [2]. These tumors were reported to be distinct from SMARCA4-mutated lung carcinomas and to have a closer molecular relationship with malignant rhabdoid tumors and SCCOHT. Because of these clinicopathological and molecular differences, these SMARCA4-inactivated thoracic tumors were termed 'SMARCA-deficient thoracic sarcoma (SMARCA4-DTS)' [2].

Previous reports of SMARCA4-DTS were mostly based on retrospective histopathological reviews with exhaustive immunohistochemical work-ups and next-generation sequencing; accordingly, the detailed clinical course of SMARCA4-DTS, including sensitivity to chemotherapy and radiotherapy, remains unclear [2,3]. Here, we report the clinical courses and molecular profiles of two cases of SMARCA4-DTS. Both patients suffered from severe skeletal related events (SREs) which required emergent surgical and radiological therapies. Severe SREs could thus be a new significant clinical feature of SMARCA4-DTS.

2. Patient 1: clinical course

A Japanese 45-year-old man visited our hospital complaining of wet cough with hemoptysis, facial swelling, and right upper leg pain. He was a current smoker with 54 pack-years. A chest X-ray and computed tomography (CT) scan revealed an 11-cm mass in the lung field and

* Corresponding author at: Department of Thoracic Oncology, Osaka International Cancer Institute, 3-1-69 Otemae Chuoku, Osaka City, 541-8567, Japan.
E-mail address: kunimasa-ke@mc.pref.osaka.jp (K. Kunimasa).
[1] These authors contributed equally to this work.

https://doi.org/10.1016/j.lungcan.2019.03.029
Received 15 January 2019; Received in revised form 20 February 2019; Accepted 26 March 2019

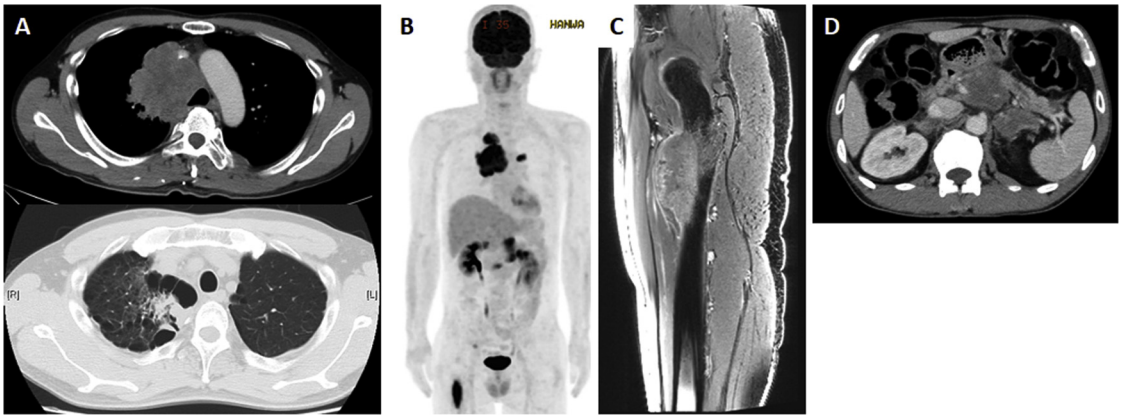

Fig. 1. Imaging features of Patient.1 (A) Contrast-enhanced computed tomography (CT) showed an intrathoracic mass adjacent to the mediastinum (upper row), as well as paraseptal emphysema, in the lung field (lower row). (B) Positron emission tomography (PET) scan revealed markedly increased ^{18}F-FDG uptake in intrathoracic lesions, as well as left adrenal and right femur metastases. (C) Magnetic resonance imaging (MRI) STIR (short T1 inversion recovery) image of right femur revealed a metastatic femur tumor and an impending pathologic fracture. (D) Contrast-enhanced CT showed enlarged abdominal lymph node metastases.

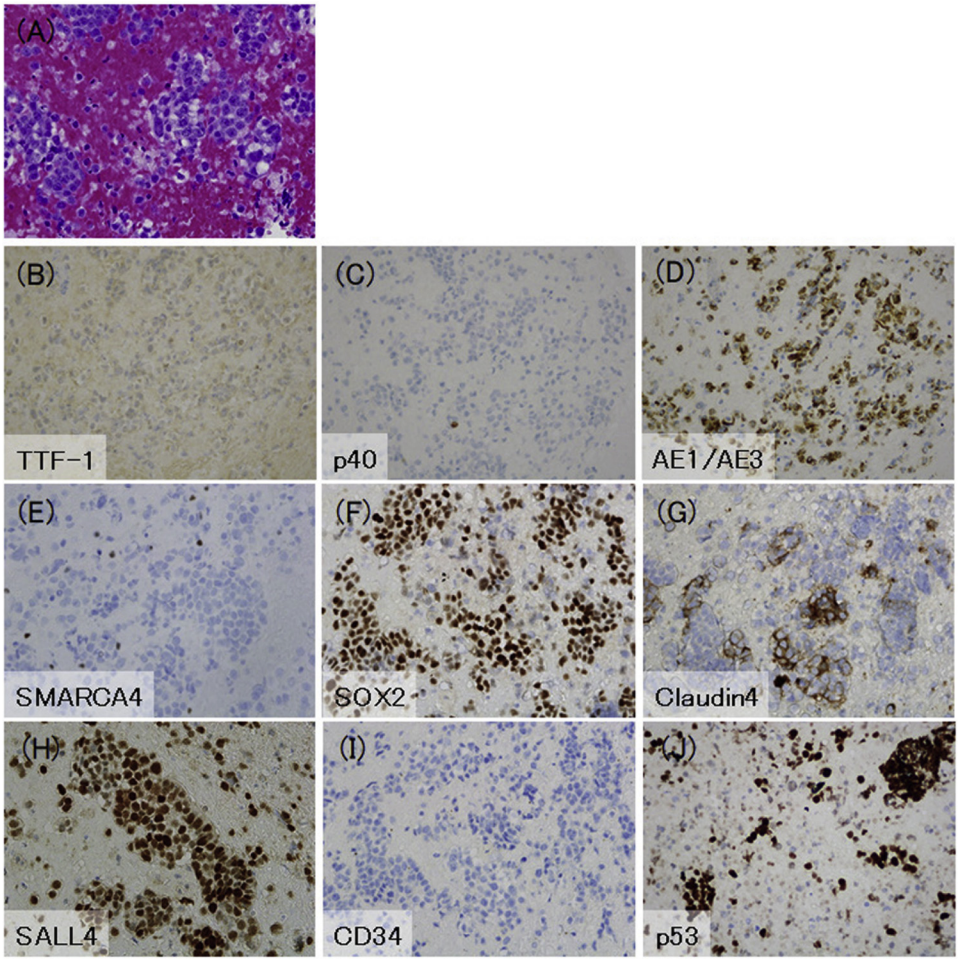

Fig. 2. Histologic and immunohistochemical features of Patient.1's specimen (A) Small- to medium-sized discohesive tumor cells with moderate nuclear atypia and prominent nucleoli and mild pleomorphism. Immunohistochemical profile: (B) TTF-1, diffusely lost in tumor cells; (C) p40, diffusely lost in tumor cells; (D) AE1/AE3, partially expressed in tumor cells; (E) SMARCA4, diffusely lost in tumor cells; (F) SOX2, diffusely expressed in tumor cells; (G) Claudin4, slightly expressed in tumor cells; (H) SALL4, expressed in tumor cells; (I) CD34, lost in tumor cells; (*J*) p53, diffusely expressed in tumor cells.

paraseptal emphysema (Fig. 1A). Positron emission tomography (PET)-CT imaging demonstrated abnormal uptakes (Fig. 1B). Endobronchial ultrasound-guided transbronchial needle aspiration was performed and histopathological analysis of the specimen revealed undifferentiated non-small cell lung carcinoma (NSCLC). An MRI scan of the right thigh revealed an impending pathologic fracture in the right femur (Fig. 1C). An *EGFR* mutation and *ALK* and *ROS1* fusions were not detected and the PD-L1 tumor proportion score (TPS) was 0%. Nab-PTX plus CBDCA therapy with concurrent radiotherapy (60 Gy/30 fr) for the mediastinal mass and intramedullary nailing fixation were respectively performed.

Table 1
Genetic alterations of Patient.1 and 0.2.

Chromosome	Gene	Transcript Variant	Protein Variant	Allele frequency (%)
Patient.1				
1	*PDE4DIP*	c.5284C > T; c.5692C > T; n.5118C > T; c.5482C > T; c.5695C > T; c.5539C > T; c.4963C > T; c.5770C > T; c.4966C > T	p.P1924S; p.P1847S; p.P1828S; p.P1899S; p.P1898S; p.P1656S; p.P1655S; p.P1762S	50.8
2	*LRP1B*	c.6461G > T	p.C2154F	45.0
2	*LRP1B*	c.1591C > T	p.R531C	49.3
3	*EPHA3*	c.1839C > T	p.A613A	85.2
4	*ADGRL3*	c.1143C > A; c.939C > A	p.A313A; p.A381A	80.8
4	*TET2; TET2-AS1*	c.5099A > G; c.5162A > G; n.318 + 58777T > C	p.N1700S; p.N1721S	82.1
5	*GDNF-AS1; GDNF*	c.124 + 65G > T; c.189G > T; c.73 + 65G > T; c.138G > T; c.-86 + 65G > T; n.1020 + 10133C > A	p.A63A; p.A46A	77.6
7	*TRRAP*	c.10176G > T; c.10263G > T; c.10230G > T	p.T3392T; p.T3410T; p.T3421T	30.8
7	*PIK3CG*	c.2386C > G	p.L796V	31.0
8	*CSMD3*	c.2788C > A; c.2866C > A; c.3058C > A; c.3178C > A	p.L1060I; p.L930I; p.L1020I; p.L956I	45.4
12	*ARID2*	c.-66C > T; c.4111C > T; c.2941C > T; c.3664C > T	p.H1371Y; p.H981Y; p.H1222Y	46.7
13	*RB1*	c.1468G > C	p.A490P	87.6
13	*FLT1*	c.1580C > A	p.S527Y	85.9
15	*BLM*	c.719A > G; c.-573A > G	p.D240G	52.1
16	*TSC2*	c.1759G > T; c.1270G > T; c.1903G > T; c.1870G > T; c.1723G > T	p.D424Y; p.D624Y; p.D635Y; p.D587Y; p.D575Y	90.9
17	*RNF213*	c.10689C > T; n.1400G > A; n.1350G > A; c.10836C > T	p.L3612L; p.L3563L	48.3
17	*TP53*	c.-906G > T; c.212G > T; c.329G > T; c.-825G > T	p.R110L; p.R71L	87.0
18	*DCC*	c.1279G > C; c.2314G > C	p.V772L; p.V427L	83.1
19	*SMARCA4*	c.896delC	p.P299fs*4	88.7
20	*SRC*	c.1080C > G; c.1098C > G	p.Y366*; p.Y360*	47.1
X	*TBX22*	c.1017C > A; c.1377C > A	p.I459I; p.I339I	99.5
Patient.2				
1	*PIK3C2B*	c.3460G > C; c.3544G > C; n.147-756C > G	p.A1154P; p.A1182P	45.6
2	*ALK*	c.1055A > G; c.-77A > G	p.H352R	74.6
3	*MLH1*	c.1945G > C; c.2017G > C; c.2110G > C; c.1903G > C; c.1816G > C;	p.V635L; p.V346L; p.V606L; p.V649L; p.V704L;	18.0
		c.1036G > C; c.1387G > C; c.2011G > C; c.1087G > C	p.V363L; p.V671L; p.V673L; p.V463L	
3	*PBRM1*	c.3185G > C; c.3293G > C; c.3173G > C; c.3089G > C;	p.R1037P; p.R1058P; p.R1077P; p.R1098P;	64.3
		c.3110G > C; c.3230G > C; c.3284G > C; c.3290G > C	p.R1097P; p.R1030P; p.R1062P; p.R1095P	
3	*AC093495.4; XPC*	c.1731G > T; c.1626 + 105G > T; n.1835G > T; n.1711G > T; c.1713G > T; n.457-7724C > A; c.1152G > T	p.W577C; p.W571C; p.W384C	70.2
6	*SYNE1*	c.8488G > T; c.8533G > T; c.8467G > T	p.D2823Y; p.D2845Y; p.D2830Y	45.5
7	*EPHB6*	c.1514C > G; n.2383C > G; c.2393C > G; c.2390C > G	p.S505C; p.S798C; p.S797C	22.2
7	*TRIM24*	c.1580A > T; c.1478A > T	p.N527I; p.N493I	45.7
9	*TAF1L*	c.4648C > T	p.P1550S	20.7
9	*PTPRD*	c.2638A > T; c.2623A > T; c.2629A > T; c.3871A > T; c.2608A > T	p.K870*; p.K880*; p.K1291*; p.K875*; p.K877*	59.8
10	*RET*	c.890G > A; c.128G > A	p.R43H; p.R297H	39.4
11	*RRM1*	c.724G > T; c.1738G > T; c.1447G > T; c.1072G > T	p.D242Y; p.D580Y; p.D358Y; p.D483Y	32.4
12	*CCND2*	n.126 + 1839G > A; n.182 + 1076G > A; c.180C > T	p.A60A	56.3
14	*BCL2L2-PABPN1*	c.233G > C	p.R78P	30.5
15	*IGF1R*	c.3985G > T; c.3988G > T; n.349-2938C > A	p.G1329C; p.G1330C	38.1
17	*TP53*	c.536A > G; c.59A > G; c.503A > G; c.419A > G; c.140A > G	p.H20R; p.H140R; p.H168R; p.H47R; p.H179R	62.4
18	*DCC*	n.218 + 5814C > T; c.4010G > A; c.2909G > A	p.R970Q; p.R1337Q	50.9
19	*SMARCA4*	c.2274G > T; c.2466G > T; n.-1177G > T	p.Q758H; p.Q822H	62.3
19	*STK11*	c.147C > G	p.Y49*	66.9
20	*GNAS*	c.*42 + 14142G > T; c.1576G > T; c.1763G > T; c.-39 + 13153G > T; c.1573G > T	p.A526S; p.A525S; p.C588F	78.5
22	MN1	c.919C > A	p.Q307K	20.0
X	TAF1	c.3319A > G; n.3458A > G; c.3382A > G	p.M1107V; p.M1128V	77.9

Mutation detection was examined using the Ion AmpliSeqTM comprehensive cancer panel (Thermo Fisher Scientific, Massachusetts, USA). Library preparation was performed according to the manufacturer's instructions. The purified libraries were pooled and then sequenced with a NextSeq 500 instrument (Illumina, San Diego, CA). Reads were aligned with the hg19 human reference genome, and variant detection was performed according to the manufacturer's pipeline (Chang Xu et al, Detecting very low allele fraction variants using targeted DNA sequencing and a novel molecular barcode-aware variant caller. BMC Genomics. 2017; 18: 5.). Germline mutations were excluded with the use of the Human Genetic Variation Database (http://www.genome.med.kyoto-u.ac.jp/SnpDB) and the Exome Aggregation Consortium database.

After two courses of chemotherapy, abdominal lymph node metastases progressed (Fig. 1D) and the second biopsy was performed. Histopathological analysis revealed an undifferentiated round cell tumor without spindle cell tumor (Fig. 2A). Immunohistochemical analysis was shown in (Fig. 2). The Ion AmpliSeq™ comprehensive cancer panel (Thermo Fisher Scientific, Massachusetts, USA) identified a frameshift mutation in P299fs (896delC) in *SMARCA4* (Table 1). Collectively, a diagnosis of SMARCA4-DTS was finally made. All following chemotherapy regimens including immune checkpoint inhibitor (ICI) failed after two courses and 11 months after the first visit, the patient died.

3. Patient 2: clinical course

A Japanese 45-year-old man visited our hospital complaining of worsening back pain. He was a current smoker with 29 pack-years. A

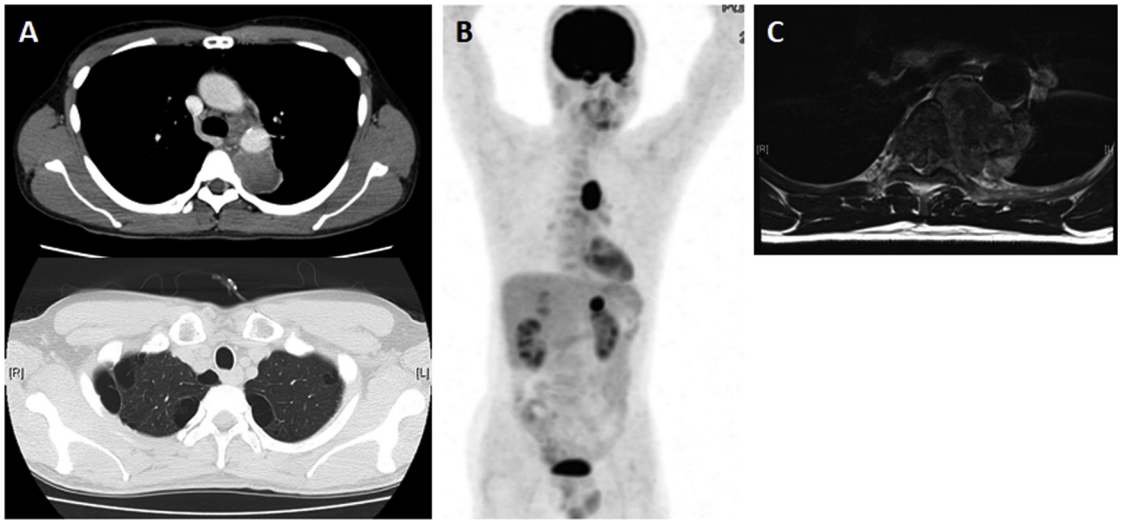

Fig. 3. Imaging features of Patient.2 (A) Contrast-enhanced computed tomography (CT) showed intrathoracic mass adjacent to the mediastinum (upper row), with paraseptal emphysema, in the lung field (lower row). (B) Positron emission tomography (PET) scan revealed markedly increased ^{18}F-FDG uptake in intrathoracic lesions and left adrenal metastasis. (C) Magnetic resonance imaging (MRI) T1-weighted image of the 5th thoracic vertebra revealed metastatic tumor invasion into the spinal cord.

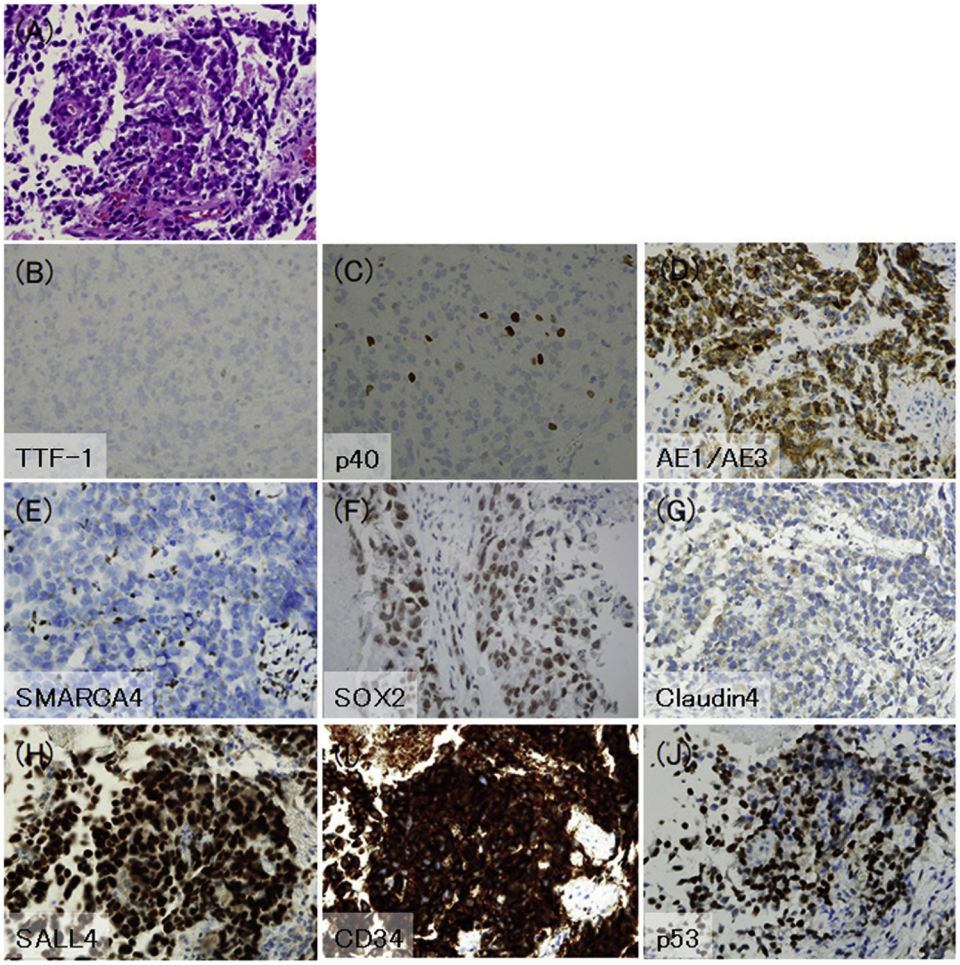

Fig. 4. Histologic and immunohistochemical features of Patient.2's specimen (A) Rhabdoid cells showing abundant eosinophilic cytoplasm and large vesicular nuclei. Immunohistochemical profile: (B) TTF-1, diffusely lost in tumor cells; (C) p40, almost diffusely lost in tumor cells; (D) AE1/AE3, partially expressed in tumor cells; (E) SMARCA4, diffusely lost in tumor cells; (F) SOX2, diffusely expressed in tumor cells; (G) Claudin4, diffusely lost in tumor cells; (H) SALL4, expressed in tumor cells; (I) CD34, lost in tumor cells; (*J*) p53, diffusely expressed in tumor cells.

chest X-ray and CT scan revealed a 5-cm mass in the lung field (Fig. 3A). PET-CT imaging demonstrated abnormal uptakes (Fig. 3B). Transbronchial lung biopsy was performed from the mass and histopathological analysis revealed undifferentiated NSCLC. The patient was diagnosed with NSCLC (cStage IV) with no *EGFR* mutation or *ALK* and *ROS1* fusion genes, and with a PD-L1 TPS of 0%. A combination therapy of CBDCA plus nab-PTX and an ICI was administered followed by ICI maintenance therapy. After two courses of maintenance therapy, the patient complained of progressive left leg weakness. An emergent MRI scan of the entire spine revealed spinal tumor compression (Fig. 3C) resulting in emergent laminectomy for decompression of the spine. Histopathological analysis revealed rhabdoid cells were focally observed without spindle cell tumor. Immunohistochemical analysis was shown in (Fig. 4). The comprehensive cancer panel sequencing identified frameshift mutations at Q758H and Q822H (2774 G > T and 2466 G > T, respectively; Table 1). Unfortunately, the emergent surgery could not improve his symptoms and eleven months after the first visit, the patient died from his cancer under palliative care, similar to Patient 1.

4. Discussion

Clinical and histological features of our cases were highly similar to those described in a previous study and exhibited sufficient characteristics to suspect SMARCA4-DTS [2,3]. Prototypical cases of SMARCA4-DTS showed the features of poorly differentiated neoplasms with epithelioid/rhabdoid cell tumors different from typical sarcoma derived from mesenchymal tissue [2]. Histopathological analysis of our cases revealed some histopathologic features associated with sarcoma including small round cell tumor (Patient. 1) and rhabdoid cell tumor (Patient. 2). Both cases showed lack of Claudin-4 expression, which distinguishes SMARCA4-DTS from SMARCA4 mutated carcinomas [4]. Our cases highlighted the fact that for the early diagnosis of SMARCA4-DTS, the integrated analysis is necessary and that SMARCA4-DTS has tends to be associated with severe SREs requiring emergent surgical and radiological treatment.

Our cases had many clinical and radiological observations in common, as follows: relatively young age of onset (mid-40 s), heavy smokers, paraseptal emphysema in the upper lung lobes, locations adjacent to the mediastinum, left adrenal metastases, and poor prognosis [2,3]. Our new clinical finding is the tendency to suffer from severe SREs. SMARCA4-DTS has a tendency to be located near the mediastinum and its rapid progression can induce direct invasion into thoracic vertebrae resulting in spinal compression. Its prognosis has been reported poor despite multidisciplinary therapy, although its detailed clinical course has not been reported. Severe SREs could negatively affect patient performance status and lead to the discontinuation of cytotoxic chemotherapy.

The diagnosis of SMARCA4-DTS is challenging. For the histopathological examination of thoracic tumors, biopsy samples are often too small to make an exact diagnosis [5]. Further, the lack of recognition of this disease makes diagnosis more difficult. Both of our cases were inadequately diagnosed at the first biopsy, whereas another larger biopsy resulted in accurate diagnoses. To obtain large specimens, other procedures than bronchoscopy including bronchoscopic cryosurgical techniques, CT-guided biopsy, and open surgical biopsy might be suitable [6]. Moreover, the clinical and radiological features of SMARCA4-DTS encourage clinicians to select other biopsy procedures for large specimen, rather than transbronchial biopsy.

Immunohistochemical screening based on SMARCA4 staining is not sufficient for the diagnosis of SMARCA4-DTS, as a loss of expression is also observed in SMARCA4-mutated lung carcinomas [2]. SOX2 staining can serve as a surrogate marker to discriminate SMARCA4-DTS from SMARCA4-mutated lung carcinomas [2,7]. Our cases showed complete loss of SMARCA4 expression and increased expression of SOX2, which was in accordance with the major SMARCA4-DTS immunohistochemical signature. Thus, immunohistochemical screening with multiple antibodies including SMARCA4 and SOX2 is necessary for the diagnosis of SMARCA4-DTS.

Moreover, molecular features are not useful in the early diagnosis. Apart from *SMARCA4*, *TP53* was found to be the only recurrently mutated gene; however, this mutation is not specific for SMARCA4-DTS and also occurs all lung carcinoma tissue types [2,3]. We analyzed molecular findings in our cases based on cancer panel sequencing covering all exons of 409 key genes and found that *TP53* mutations were common (Table 1). Heavy smoking history is considered to be a major cause of SMARCA4-DTS. *TP53* and *STK11* (Patient. 2) mutations are driver mutations associated with smoking in lung cancer [8]. Immunohistochemical loss of SMARCA4 expression suggested a nonsense mutation in the gene. For the diagnostic sequencing proof of the nonsense mutation might not be necessary; however, the clinicopathological and molecular features of SMARCA4-DTS have not been fully elucidated and its diagnostic criteria have not been established. Thus, additional molecular features of SMARCA4-DTS are necessary to understand the pathological background; moreover, not only cancer panel sequencing, but also whole exome sequencing, will be expected despite its expensive cost.

The underlying mechanism of how inactivation of the SWI/SNF complex including SMARCA4 induces tumorigenesis has been partially unraveled. The SWI/SNF complex functions as an inhibitor of the prooncogenic transcriptional coactivators YAP and TAZ [9]. Recently, targeted therapy for SWI/SNF complex mutations has been developed. Specifically, inhibition of the histone methyltransferase EZH2 has shown a growth inhibitory effect for a subset of SWI/SNF complex mutations [10]. Moreover, SMARCA4-mutant NSCLC cell lines were reported to be sensitive to Aurora kinase A inhibition [11]. Another recent study highlighted the fundamental role of the SWI/SNF complex in facilitating the efficient genes required for energy generation. This study demonstrated the complex metabolic rewiring that occurs in SWI/SNF-mutant lung adenocarcinoma, which results in the increased reliance on oxidative phosphorylation (OXPHO) and the marked sensitivity to OXPHO inhibition by the novel small molecule IACS-010759, currently under clinical development [12]. These emerging drugs have the potential to improve prognosis for SMARCA4-DTS patients.

The identification of SMARCA4-DTS is important both prognostically and therapeutically. These tumors behave aggressively and are associated with a worse prognosis. However, the diagnosis of SMARCA4-DTS is sometimes challenging. Accordingly, clinicians and pathologists are encouraged to be aware of this new entity and consider additional ancillary tests to yield a definitive diagnosis. Although clinical cues including young age onset, heavy smoking history, paraseptal pulmonary emphysema and tumor location adjacent to the mediastinum are significantly important, the diagnosis of SMARCA4-DTS relies on pathological analysis. The histopathologic features of SMARCA4-DTS are not specific but distinctive enough to infer the diagnosis [7]. The characteristic features of SMARCA4-DTS are the presence of small round to epithelioid cells in a solid pattern showing rhabdoid differentiation [3,7]. In the practical clinical setting, immunohistochemical features of undifferentiated/dedifferentiated lung carcinomas, for example lacking of TTF-1, p40 expression, also contributes to the appropriate workup for the diagnosis. Moreover immunohistochemical screening for expression of SMARCA4 could be useful especially when dealing with small biopsy samples. [7]. Currently, we do not have effective treatments for SMARCA4-DTS; however the potential development of targeted therapy for this disease provides additional clinical relevance for the identification of SMARCA4-DTS. In conclusion, an integrated clinico-radiologic–pathologic–genetic diagnosis is essential for the diagnosis of this disease.

Funding

There is no funding support about this study.

Ethical approval

This article does not contain any studies with human participants or animals performed by any of the authors.

Informed consent

Informed consent was obtained from the present two patients in the study.

Conflict of interest

The authors have no conflicts of interest to disclose concerning the study.

References

[1] C. Kadoch, D.C. Hargreaves, C. Hodges, et al., Proteomic and bioinformatic analysis of mammalian SWI/SNF complexes identifies extensive roles in human malignancy, Nat. Genet. 45 (2013) 592–601.
[2] F. Le Loarer, S. Watson, G. Pierron, et al., SMARCA4 inactivation defines a group of undifferentiated thoracic malignancies transcriptionally related to BAF-deficient sarcomas, Nat. Genet. 47 (2015) 1200–1205.
[3] A. Yoshida, E. Kobayashi, T. Kubo, et al., Clinicopathological and molecular characterization of SMARCA4-deficient thoracic sarcomas with comparison to potentially related entities, Mod. Pathol. 30 (2017) 797–809.
[4] I.M. Schaefer, A. Agaimy, C.D. Fletcher, et al., Claudin-4 expression distinguishes SWI/SNF complex-deficient undifferentiated carcinomas from sarcomas, Mod. Pathol. 30 (2017) 539–548.
[5] S. Kuwamoto, M. Matsushita, K. Takeda, et al., SMARCA4-deficient thoracic sarcoma: report of a case and insights into how to reach the diagnosis using limited samples and resources, Hum. Pathol. 70 (2017) 92–97.
[6] A. Babiak, J. Hetzel, G. Krishna, et al., Transbronchial cryobiopsy: a new tool for lung biopsies, Respiration 78 (2009) 203–208.
[7] R. Perret, L. Chalabreysse, S. Watson, et al., SMARCA4-deficient thoracic sarcomas: clinicopathologic study of 30 cases with an emphasis on their nosology and differential diagnoses, Am. J. Surg. Pathol. (November (16)) (2018), https://doi.org/10.1097/PAS.0000000000001188.
[8] A. Karlsson, M. Ringnér, M. Lauss, et al., Genomic and transcriptional alterations in lung adenocarcinoma in relation to smoking history, Clin. Cancer Res. 20 (2014) 4912–4924.
[9] L. Chang, L. Azzolin, D. Di Biagio, et al., The SWI/SNF complex is a mechanoregulated inhibitor of YAP and TAZ, Nature 563 (2018) 265–269.
[10] C.M. Fillmore, C. Xu, P.T. Desai, et al., EZH2 inhibition sensitizes BRG1 and EGFR mutant lung tumours to TopoII inhibitors, Nature 520 (2015) 239–242.
[11] V. Tagal, S. Wei, W. Zhang, et al., SMARCA4-inactivating mutations increase sensitivity to Aurora kinase A inhibitor VX-680 in non-small cell lung cancers, Nat. Commun. 19 (January (8)) (2017) 14098.
[12] Y. Lissanu Deribe, Y. Sun, C. Terranova, et al., Mutations in the SWI/SNF complex induce a targetable dependence on oxidative phosphorylation in lung cancer, Nat. Med. 24 (2018) 1047–1057.